Pulsed quantum cascade laser-based CRDS substance detection: real-time detection of TNT

C. C. Harb,[1,*] T. K. Boyson,[1] A. G. Kallapur,[1] I. R. Petersen,[1] M. E. Calzada,[2] T. G. Spence,[2] K. P. Kirkbride,[3] and D. S. Moore[4]

[1]*School of Engineering and Information Technology, University College, The University of New South Wales, Canberra, ACT 2600, Australia*
[2]*Department of Mathematical Sciences and Department of Chemistry, Loyola University New Orleans, New Orleans, LA 70118, USA*
[3]*Forensic and Data Centres, Australian Federal Police, Weston, ACT 2611, Australia*
[4]*Shock and Detonation Physics Group, Los Alamos National Lab, Los Alamos, NM 87545, USA*
[*]*c.harb@adfa.edu.au*

Abstract: This paper presents experimental results from a pulsed quantum cascade laser based cavity ringdown spectrometer used as a high-throughput detection system. The results were obtained from an optical cavity with 99.8% input and output coupling mirrors that was rapidly swept (0.2s to 7s sweep times) between 1582.25 cm^{-1} (6.3201μm) and 1697.00 cm^{-1} (5.8928μm). The spectrometer was able to monitor gas species over the pressure range 585 torr to 1μtorr, and the analysis involves a new digital data processing system that optimises the processing speed and minimises the data storage requirements. In this approach we show that is it not necessary to make direct measurements of the ringdown time of the cavity to obtain the system dynamics. Furthermore, we show that correct data processing is crucial for the ultimate implementation of a wideband IR spectrometer that covers a range similar to that of commercial Fourier transform infrared instruments.

OCIS codes: (300.1030) Absorption; (300.6340) Spectroscopy, infrared; (300.6360) Spectroscopy, laser; (120.6200) Spectrometers and spectroscopic instrumentation; (260.3060) Infrared.

References and links

1. D. Moore, "Instrumentation for trace detection of high explosives," Rev. Sci. Instrum. **75**, 2499–2512 (2004).
2. D. S. Moore, "Recent advances in trace explosives detection instrumentation," Sens. Imaging **8**, 9–38 (2007).
3. B. A. Paldus, C. C. Harb, T. G. Spence, R. N. Zare, C. Gmachl, F. Capasso, D. L. Sivco, J. N. Baillargeon, A. L. Hutchinson, and A. Y. Cho, "Cavity ringdown spectroscopy using mid-infrared quantum-cascade lasers," Opt. Lett. **25**, 666–668 (2000).
4. R. F. Curl, F. Capasso, C. Gmachl, A. A. Kosterev, B. McManus, R. Lewicki, M. Pusharsky, G. Wysocki, and F. K. Tittel, "Quantum cascade lasers in chemical physics," Chem. Phys. Lett. **487**, 1–18 (2010).
5. F. Capasso, "High-performance midinfrared quantum cascade lasers," Opt. Eng. **49**, 111102 (2010).
6. M. B. Pushkarsky, I. G. Dunayevskiy, M. Prasanna, A. G. Tsekoun, R. Go, and C. K. N. Patel, "High-sensitivity detection of TNT," Proc. Natl. Acad. Sci. U.S.A. **103**, 19630–19634 (2006).
7. G. Hancock, S. J. Horrocks, G. A. D. Ritchie, J. H. van Helden, and R. J. Walker, "Time-resolved detection of the CF_3 photofragment using chirped QCL radiation," J. Phys. Chem. A **112**, 9751–9757 (2008).
8. J. H. van Helden, R. Peverall, G. A. D. Ritchie, and R. J. Walker, "Rapid passage effects in nitrous oxide induced by a chirped external cavity quantum cascade laser," Appl. Phys. Lett. **94**, 051116 (2009).

#165708 - $15.00 USD Received 29 Mar 2012; revised 15 May 2012; accepted 12 Jun 2012; published 25 Jun 2012

9. D. S. Sayres, E. J. Moyer, T. F. Hanisco, J. M. St. Clair, F. N. Keutsch, A. O'Brien, N. T. Allen, L. Lapson, J. N. Demusz, M. Rivero, T. Martin, M. Greenberg, C. Tuozzolo, G. S. Engel, J. H. Kroll, J. B. Paul, and J. G. Anderson, "A new cavity based absorption instrument for detection of water isotopologues in the upper troposphere and lower stratosphere," Rev. Sci. Instrum. **80**, 044102 (2009).
10. P. C. Kuffner, K. J. Conroy, T. K. Boyson, G. Milford, A. G. Kallapur, I. R. Petersen, M. E. Calzada, T. G. Spence, K. P. Kirkbride, and C. C. Harb, "Quantum cascade laser-based substance detection: approaching the quantum noise limited," Proc. SPIE **8032**, 80320C-1–80320C-10 (2011).
11. P. R. Griffiths and J. A. De Haseth, *Fourier Transform Infrared Spectrometry*, 2nd. ed. (Wiley-Interscience, Hoboken, NJ, USA, 2007).
12. K. W. Busch and M. A. Busch, *Cavity-Ringdown Spectroscopy: An Ultratrace-Absorption Measurement Technique* (ACS Symp. Ser. 720, American Chemical Society, Washington, DC, 1999).
13. G. Berden, R. Peeters, and G. Meijer, "Cavity ringdown spectroscopy: experimental schemes and application," Int. Rev. Phys. Chem. **19**, 565–607 (2000).
14. M. W. Todd, R. A. Provencal, T. G. Owano, B. A. Paldus, A. Kachanov, K. L. Vodopyanov, M. Hunter, S. L. Coy, J. I. Steinfeld, and J. T. Arnold, "Application of mid-infrared cavity ringdown spectroscopy to trace explosives vapor detection using a broadly tunable (68 μm) optical parametric," Appl. Phys. B **75**, 367–376 (2002).
15. A. O'Keefe and D. A. G. Deacon, "Cavity ringdown optical spectrometer for absorption measurements using pulsed laser sources," Rev. Sci. Instrum. **59**, 2544–2551 (1988).
16. J. Xie, B. A. Paldus, E. H. Wahl, J. Martin, T. G. Owano, C. H. Kruger, J. S. Harris, and R. N. Zare, "Near-infrared cavity ringdown spectroscopy of water vapor in an atmospheric flame," Chem. Phys. Lett. **284**, 387–395 (1998).
17. A. A. Istratov and O. F. Vyvenko, "Exponential analysis in physical phenomena," Rev. Sci. Instrum. **70**, 1233–1257 (1999).
18. M. Mazurenka, R. Wada, A. J. L. Shillings, T. J. A. Butler, J. M. Beames, and A. J. Orr-Ewing, "Fast fourier transform analysis in cavity ring-down spectroscopy: application to an optical detector for atmospheric NO_2," Appl. Phys. B **81**, 135–141 (2005).
19. M. A. Everest and D. B. Atkinson, "Discrete sums for the rapid determination of exponential decay constants," Rev. Sci. Instrum. **79**, 023108 (2008).
20. A. G. Kallapur, I. R. Petersen, T. K. Boyson, and C. C. Harb, "Nonlinear Estimation of a Fabry-Perot Optical Cavity for Cavity Ring-Down Spectroscopy," in *IEEE Intern. Conf. on Cont. Applic. (CCA)*, (Yokohama, Japan) (2010), pp. 298–303.
21. A. G. Kallapur, T. K. Boyson, I. R. Petersen, and C. C. Harb, "Nonlinear estimation of ring-down time for a Fabry-Perot optical cavity," Opt. Express **19**, 6377–6386 (2011).
22. A. G. Kallapur, I. R. Petersen, T. K. Boyson, and C. C. Harb, "Robust nonlinear estimation for a Fabry-Perot optical cavity," *in 8th Asian Control Conference* (Kaohsiung, Taiwan) (2011), pp. 1454–1459.
23. T. K. Boyson, T. G. Spence, M. E. Calzada, and C. C. Harb, "A frequency domain analysis method for cavity ring-down spectroscopy," Opt. Express **19**, 8092–8101 (2011).
24. D. Z. Anderson, J. C. Frisch, and C. S. Masser, "Mirror reflectometer based on optical cavity decay time," Appl. Opt. **23**, 1238–1245 (1984).
25. D. Z. Anderson, "Reflectometer based on optical cavity decay time," U.S. patent 4,571,085 (February 18, 1986).
26. B. J. Orr and Y. He, "Rapidly swept continuous-wave cavity-ringdown spectroscopy," Chem. Phys. Lett. **512**, 1–20 (2011).
27. Database, *National Institute of Advanced Industrial Science and Technology (AIST)*, Japan. `http://riodb01.ibase.aist.go.jp/sdbs/cgi-bin/direct_frame_top.cgi`, (2011).
28. R. W. Beal and T. B. Brill, "Vibrational behavior of the - NO_2 group in energetic compounds," Appl. Spect. **59**, 1194–1202 (2005).

1. Introduction

The detection of substances that pose chemical, biological and explosives (CBE) threats has become critical to security agencies worldwide. In recent years there have been many advances in instrumentation designed for trace detection [1, 2]. These instruments have been constructed to address the needs of security and law enforcement agencies that are determined to locate illicit compounds. A major hindrance in this endeavour has been to measure the compounds of interest given their low concentrations. Hence, great interest has recently developed in strategies that can enhance the signal from species of interest while simultaneously reducing sensitivity to contaminants.

The molecules of interest for this research area are often heavy molecules and have complicated quantum structures, such as TNT, RDX, etc. Other molecules, such as, N_2, O_2, CO_2,

#165708 - $15.00 USD Received 29 Mar 2012; revised 15 May 2012; accepted 12 Jun 2012; published 25 Jun 2012

H_2O, etc, that are common in the atmosphere also have spectra in the investigated wavelength range and act to mask the species of interest. The combination of all these molecules results in absorption spectra with many rotational and vibrational states that can overlap each other. Many of the absorbing quantum transitions typically occur in the infrared wavelength range called the molecular fingerprinting wavelength range, between 4μm (2500 cm^{-1}) and 12μm (833 cm^{-1}), which can be accessed by newly developed quantum cascade lasers (QCL).

The QCL has been growing increasingly in its applicability to spectroscopic absorption measurements and is now recognised as an invaluable tool in this research area [3–5]. Although many articles have been written about the use of QCLs for spectroscopic detection there are still considerable developments required to see their deployment in general applications. Many recent studies have utilised these lasers for absorption spectroscopy, see for example [6–9], and discovered that they can be used in very interesting ways, such as intrapulse mode spectroscopy, due to the complicated scanning behaviour of these lasers. The work presented here concentrates on the cavity ringdown spectroscopy (CRDS) technique, as opposed to complimentary techniques such as integrated cavity output spectroscopy (ICOS), because the CRDS instrument can be reduced to a small size for applications that require portability due to the beam path being on axis. Secondly, the molecules under investigation have very broad absorption profiles, see [6] for example, that are much wider than the laser linewidth, and hence the other techniques have no advantage over the CRDS approach.

Figure 1 shows some of the main components that are required to successfully produce a wideband laser based spectrometer [10] capable of measuring these quantum transitions. Unlike traditional wideband instruments such as the Fourier transform infrared (FTIR) spectrometers [11], this laser-based system requires several features to construct a high resolution spectrum, that at present are not commercially available. A laser is required, instead of the thermal source in an FTIR, that can be frequency tuned over this vast wavelength range: as yet no single inexpensive source is available. Furthermore, the spectrometer requires a high finesse optical cell (cavity) that is vacuum compatible with suitable photodetectors. Although the optical coating technology does exist to make high finesse cavities in this wavelength range, no single set of mirrors are available to cover the entire range of wavelength.

The system proposed in Fig. 1 is a derivative of cavity ringdown spectroscopy (CRDS) [12–14] which is a laser-based direct-absorption technique. In CRDS, light generated by a laser is trapped in a detection cavity with high reflectivity. The intensity of the detected signal decays exponentially according to the relation $I_0 e^{-t/\tau} + O$, where I_0 is the initial intensity of the light, O represents the DC offset of the system, and τ is the cavity ringdown time which can be used to generate a spectrum for a given sample. CRDS offers a significant increase in sensitivity, sufficient to permit detection of organic explosives in the vapour phase. However, there are several drawbacks when using CRDS, which are addressed in this paper.

The other important components shown in Fig. 1 are the data acquisition system (DAQ); the control system and electronics to produce signals that can be used to adjust the system parameters; the digital to analog converters and amplifiers to drive the system components such as the laser piezo electric transducers (PZTs). Additionally, new data processing techniques are required to extract the information from the DAQ to produce an estimate for the cavity ringdown time τ, which can in turn be used to rapidly generate a spectrum, and consequently to detect the absorbing species in the sample. The challenge of this type of spectrometer lies in the quantity of data that needs to be processed to produce a spectrum [10].

This paper discusses the development of a novel cavity-enhanced pulse spectrometer. In particular, we discuss the use of commercially available components to build a test bed on which we apply new digital signal processing techniques that will ultimately allow us to construct a wideband laser-based spectrometer in the molecular fingerprinting wavelength range.

#165708 - $15.00 USD Received 29 Mar 2012; revised 15 May 2012; accepted 12 Jun 2012; published 25 Jun 2012

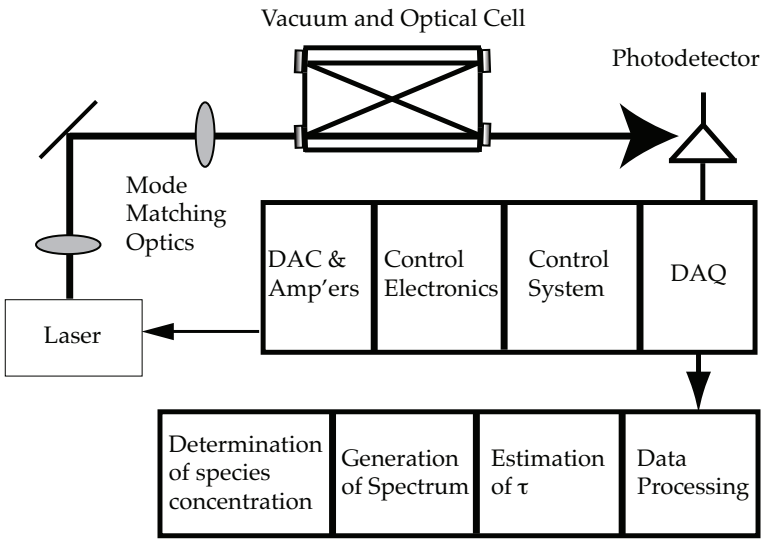

Fig. 1. Components of a laser-based wideband spectrometer.

We discuss the system requirements and maximum signal-to-noise ratio (SNR) that can be achieved. We also discuss the characteristics of the available QCL and Mercury Cadmium Telluride (MCT) detectors, the progress on the CRDS system we are developing, and the digital signal processing techniques to be used to extract the absorption data.

In section 2 we discuss the theory applicable to the digital signal processing of a repetitive CRD data, and we outline two approaches for data reduction. In section 3 we discuss the properties of the QCL system, including the noise characteristics and the coupling to the vacuum system. Finally in section 4 we present results of the QCL pulsed laser spectrometer operating in single pass, Sec. 4.1, and a real-time scanning spectrometer (i.e. a spectrum gathered at the laser scan rate) employing the harmonic data extraction technique, Sec. 4.2.

2. Theory: digital signal processing of a repetitive CRD signal

Figure 1 shows the basic configuration for a laser-based wideband spectrometer that could cover the same spectral wavelength region as a standard FTIR. However, the system requirements for a laser-based system are fundamentally different to that of an FTIR. In this system depicted by Fig. 1, a control loop and an estimation loop are required. The control loop is used to control the laser and cavity scan dynamics so that efficient intensity buildup in the cavity and ringdowns can be achieved. Under pulsed laser operation the control system simply scans the laser through its tuning range. If CW laser operation were used instead then the control loop would also need to make corrections to the laser and cavity such that they are in continuous lock throughout the scanning process.

The estimation loop can be considered to be a channel that is used to determine the ringdown time, τ, (or an equivalent quantity) as a function of wavelength, and hence the absorption spectrum. Section 2.1 outlines some issues relating data processing of the digitised signal and recent advances in solving associated technical difficulties.

2.1. Real-time determination of τ

Conventional linear least square techniques can be used to estimate the value for τ; See e.g., O'Keefe *et. al.* [15] and Xie *et. al.* [16], but such methods are susceptible to the system's noise

#165708 - $15.00 USD Received 29 Mar 2012; revised 15 May 2012; accepted 12 Jun 2012; published 25 Jun 2012

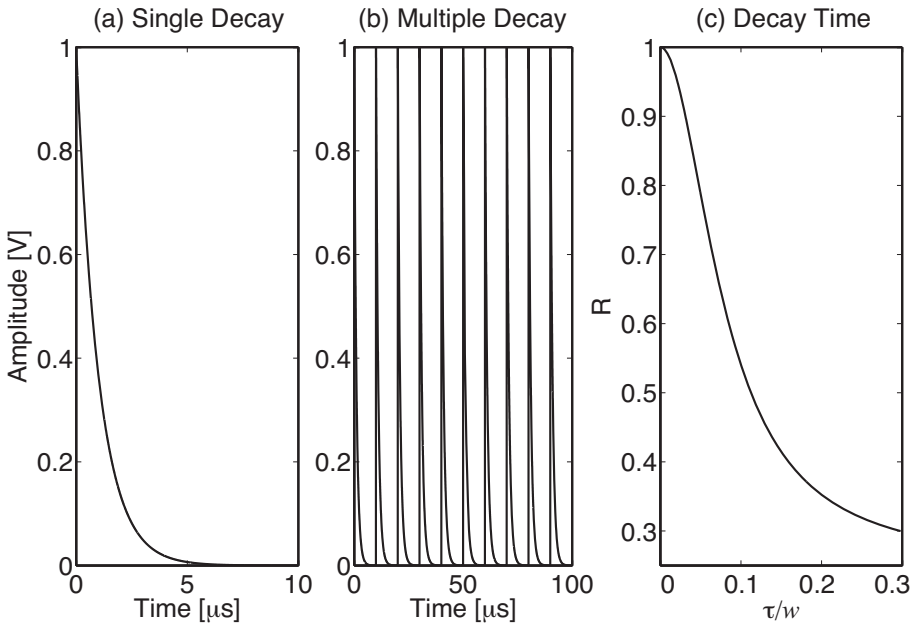

Fig. 2. Diagram of (a) Single exponential decays, (b) 10 consecutive exponential decays and (c) relationship between τ and R as a function of the data collection window w.

characteristics and instrument offsets as mentioned in Istratov *et. al.* [17] and Mazurenka *et. al.* [18]. On the other hand, nonlinear least square methods such as the Levenberg-Marquardt (LM) technique can effectively handle system noise but are known to limit the data throughput to below 10Hz as mentioned by Everest *et. al.* [19].

Taking these issues into account, we have recently proposed the use of two other techniques to determine a value of τ. The first one is a time-domain approach involving the application of a discrete-time extended Kalman filter (EKF) to estimate the value for τ [20]. We have also demonstrated the offline application of the EKF to estimate the value for τ for a set of experimentally obtained cavity ringdown data for a Fabry-Perot optical cavity [21], where it was noted that the EKF estimation results in an estimate for τ that converges to the neighbourhood of its expected true value within nine ringdown cycles. The results can be further improved by considering modelling uncertainties associated with the dynamics of the cavity and implementing robust estimation schemes. Furthermore. we have shown that a discrete-time robust EKF can be used to estimate the value for τ in the presence of general modelling uncertainties in addition to exogenous noise sources [22].

In a second approach, we have also shown that real-time processing of the data is possible, with high accuracy, using a frequency domain analysis technique [23]. This method analysed the output of the spectrometer as a whole, rather than just analysing individual ringdown transients. Simulations of the technique, comparing it to LM non-linear least squares fitting, and using a cavity locked CRDS instrument for proof-of-principle tests [23] show results that determine a value for τ 500 times faster than equivalent LM techniques.

2.2. Harmonic data extraction for τ

In this section we outline the harmonic data extraction for τ used in this work. Following the approach outlined by Boyson *et. al.* [23], we can obtain an expression for τ relative to the magnitudes of the fundamental and first harmonic frequency components of the pulse.

#165708 - $15.00 USD Received 29 Mar 2012; revised 15 May 2012; accepted 12 Jun 2012; published 25 Jun 2012

In this study, we collected and analysed ten consecutive exponential decays as shown in Fig. 2. We used the following mathematical model for our signal

$$S(t) = \sum_{k=1}^{10} S_k(t),\ 0 \le t \le 10w,$$

where

$$S_k(t) = \begin{cases} I_0 e^{-(t-(k-1)w)/\tau} + O & \text{if} \quad (k-1)w \le t \le kw \\ 0 & \text{otherwise} \end{cases}$$

Here, w is the sampling window for a single decay. Multiplying $S(t)$ with $\cos(2\pi\frac{t}{w})$ and $\cos(4\pi\frac{t}{w})$ and integrating between 0 and $10w$ results in

$$\begin{aligned} A_1 &= \int_0^{10w} S(t)\cos(2\pi\frac{t}{w})dt = 10\int_0^{w}(I_0 e^{-t/\tau} + O)\cos(2\pi\frac{t}{w})dt \\ &= -10I_0\tau w^2\frac{e^{-\frac{w}{\tau}}-1}{w^2+4\pi^2\tau^2} \end{aligned}$$

and

$$\begin{aligned} A_2 &= \int_0^{10w} S(t)\cos(4\pi\frac{t}{w})dt = 10\int_0^{w}(I_0 e^{-t/\tau} + O)\cos(4\pi\frac{t}{w})dt \\ &= -10I_0\tau w^2\frac{e^{-\frac{w}{\tau}}-1}{w^2+16\pi^2\tau^2}. \end{aligned}$$

Furthermore, we have

$$R = \frac{A_2}{A_1} = \frac{w^2+4\pi^2\tau^2}{w^2+16\pi^2\tau^2}. \tag{1}$$

Equation (1) can be solved for τ giving

$$\tau = \frac{w}{2\pi}\sqrt{\frac{1-R}{4R-1}}. \tag{2}$$

We note that this technique is independent of the initial light intensity I_0 and the DC offset O and that it can be applied to the analysis of any number of exponential decays (not just 10 ringdowns) as Eqs. (1) and (2) relate w, R, and τ only. Furthermore, w can be adjusted to ensure that the empty cavity value for τ is greater than $4R$ and hence in the stable region.

The absorbance, A, can then be determined from the relation:

$$A = -\log(\mathscr{T}) = \log\left(\frac{I_0}{I}\right) = \frac{n\times l}{2.303\times c}\left(\frac{1}{\tau}-\frac{1}{\tau_0}\right). \tag{3}$$

Where $\mathscr{T}$ is the transmittance, I is the transmitted intensity, n is the index of refraction within the optical cavity, l is the optical path length in the cavity, c is the speed of light, and τ_0 is the empty cavity decay lifetime.

3. Experimental setup and components

In this section, we outline the characteristics of the pulsed QCL system that is used in this research. Since the initial invention and reported measurement of the cavity decay constant by Anderson *et. al.* [24, 25], cavity ringdown systems have had many improvements. However, in general, the process for measuring the decay time τ has relied on the fitting of the decay signal

#165708 - $15.00 USD Received 29 Mar 2012; revised 15 May 2012; accepted 12 Jun 2012; published 25 Jun 2012

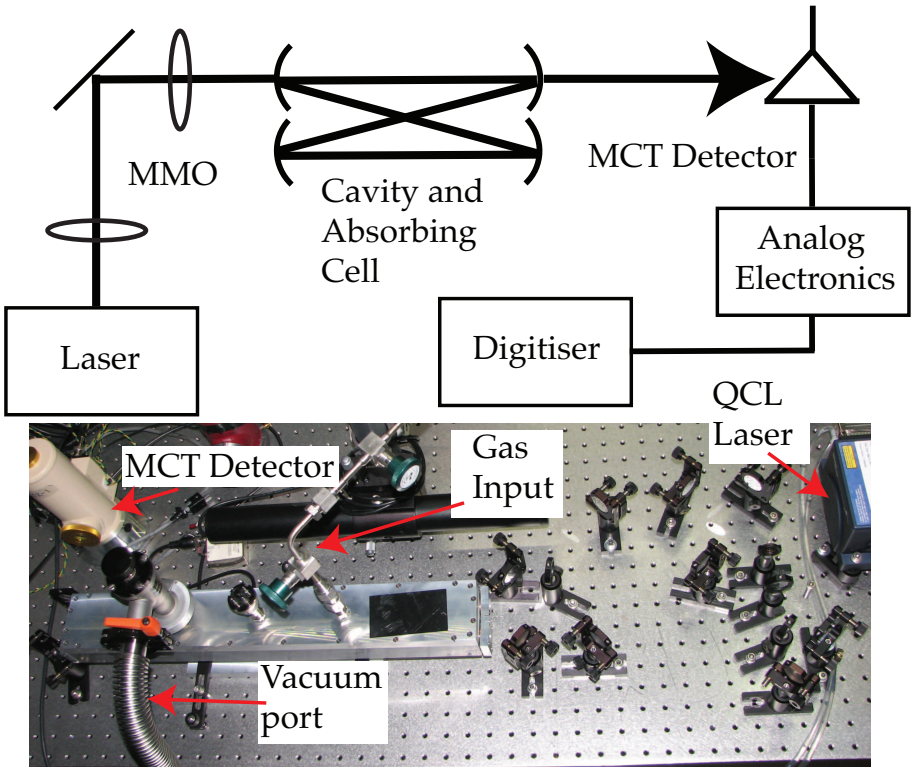

Fig. 3. LANL experimental setup for the pulsed laser measurements.

by digitising the measured decay and computing τ from the resultant parameters, but some analog techniques have also been developed, see for example [26].

Figure 3 shows the setup of our pulsed CRDS system. The system consisted of the laser, mode matching optics (MMO), alignment mirrors, the CRDS vacuum system (labelled cavity and Absorbing cell), an MCT photodetector, analog electronics to process the signals and a data acquisition (DAQ) system (labelled Digitiser).

The decay time measurement can be achieved by incorporating a nonlinear curve fitting routine, such as a Levenberg-Marquardt (LM) algorithm, to the signals measured by the MCT. The three parameters need for this process are the initial intensity I_0, the DC offset, and τ. This process requires a fast digitiser (usually $>$100 MS/s) that has many bits of resolution ($>$ 10bits if possible). For standard pulsed CRDS measurements this approach makes a lot of sense as the laser repetition rate is usually of the order of a few Hertz, which means that the laser is the limiting factor and not the characteristics of the data acquisition (DAQ). In the case of the QCL, however, the repetition rate is more like 100kHz, which changes the limiting factor of the DAQ and processing rate [10]. For example, data acquired for one second at the rate of 100MS/s using a 10bit digitising system would result in a 1Gbit file containing 10^5 ringdown events. This amount of data is difficult to deal with, even with the fastest fitting routines applied to exponential decays, the amount of data increases with either the number of bits used by the digitiser or the DAQ sampling rate. In such cases, the fitting routines have to ignore ringdown data that cannot be handled within the time available for real-time processing.

The light exiting the CRD Cavity was focused on a Kolmar KMPV8-1-J1/DC MCT detector (noise performance shown in [10]), which is an integrated high frequency infrared detector/amplifier sensor with wavelength range from 2μm (5000 cm^{-1}) to 12μm (833 cm^{-1}).

#165708 - $15.00 USD Received 29 Mar 2012; revised 15 May 2012; accepted 12 Jun 2012; published 25 Jun 2012

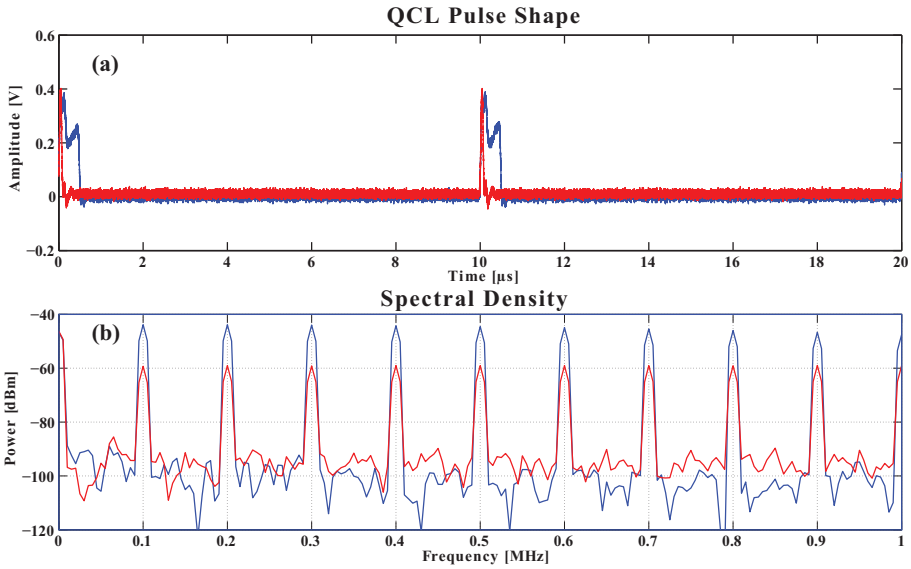

Fig. 4. (a) Pulse train signal of the Daylight Solutions tunable mid-IR external cavity laser system; (b) Power spectral density of (a).

The MCT photodiode is coupled to an internal DC to 20MHz bandwidth transimpedance amplifier. The output is both AC as well as DC and it has a broadband $D^{\star} > 1 \times 10^{10}$. The Dewar is side-looking with a 12 hour hold time and has an IR window made from ZnSe anti-reflection coated for 2μm to 13μm wavelength band.

A Daylight Solutions tunable mid-IR external cavity laser system (Model TLS-21060 Tuneable QCL with model 1001-TLC controller CW/Pulsed) was used in this investigation. In the CW case, the maximum power from the QCL was measured to be 25mW at 6.12μm. In the pulsed mode, however, the average power dropped to $\approx$ 2mW.

Figure 4(a) shows the time domain characteristics of the QCL operating with a 100ns pulse width (red) and 500ns pulse width (blue), both operating with 100kHz pulse rate. Figure 4(b) is the power spectral density of the pulse train and shows that the signal to noise ratio, SNR, is large for both cases.

The vacuum and optical cavity system used in this investigation is shown in Fig. 3. We designed the optical cavity using a four mirror configuration, i.e. a ring or figure of eight shape. The mirrors were arranged such that an O-ring was sandwiched between the aluminium spacer and the mirrors, and thus provided the vacuum seal. A backing plate, made also of aluminium, was used to hold the mirrors firmly in place.

The optical cavity consisted of one input and one output mirror, that each had a reflectivity of 99.8 %, from II-VI Infrared, with unknown transmissivity and loss. The other two mirrors were quoted to have a reflectivity of 99.995 %, from Los Gatos Research, also with an unknown transmissivity and loss. All four mirrors were plano/concave, 1" in diameter, an ROC of 1m, and were made from a ZnSe substrate.

The angle of incidence on each mirror was 2^{o} and the spacing between the mirrors was 0.5m, making a optical perimeter of $\approx$ 2m. The free spectral range of the optical cavity was therefore 150MHz; and the beam waist diameter within the cavity was 918 μm, assuming a Gaussian TEM_{00} mode.

In addition to the laser and optical cavity, a set of optics were used to mode match one to the other. The QCL waist was placed 1.75m from the waist position inside the optical cavity. Using

#165708 - $15.00 USD Received 29 Mar 2012; revised 15 May 2012; accepted 12 Jun 2012; published 25 Jun 2012

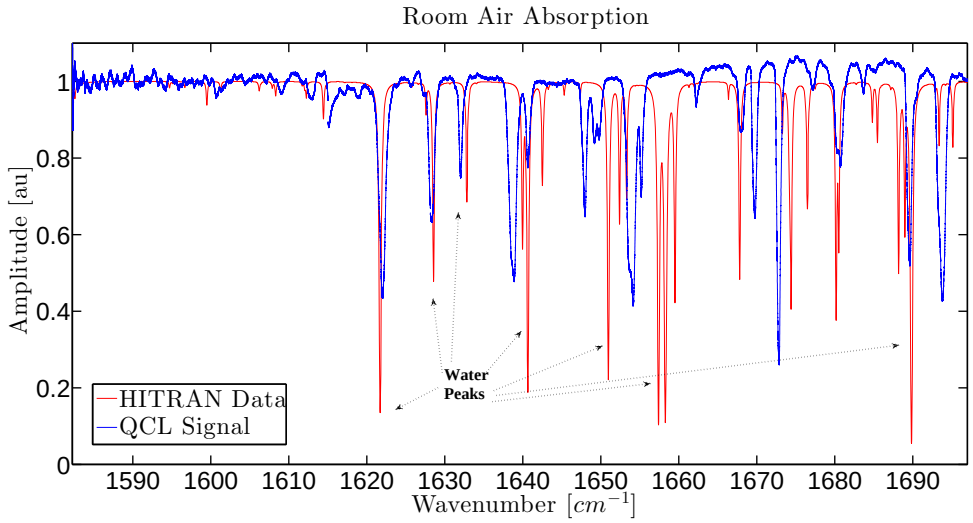

Fig. 5. Measurement of ≈ 1m room air at 1 atmosphere (at 7500ft. elevation above sea level) using the QCL (blue) compared to the HITRAN data base (red). The QCL data has been normalised by the laser intensity at each wavelength.

two plano-convex CaF_2 lenses, mode matching of the QCL to the waist of the optical cavity was achieved with a 100mm focal length lens followed by a 250mm focal length lens.

The vacuum system used an Agilent (Varian) V70 turbo pump and the cell pressure was measured using a Varian 802-A thermocouple gauge with MDC type 5310 TC gauge head.

4. Results and discussion

Figure 5 shows results obtained from the QCL passing through ≈ 1m air in the laboratory at room pressure, compared to the HITRAN data base. The predominant signal in this wavelength range is H_2O as determined from the HITRAN database, but there are other absorbers (CO_2, N_2O, NO, etc) in this range with much smaller absorption coefficients.

The results show that the qualitative features agree between the two spectra, but the absolute wavelength positions do not agree. This could be for several reasons, but most likely it is due to the scan linearity of the QCL.

In this section, we present results of the pulsed QCL setup that was operated in two modes:

1. QCL pulsed laser spectrometer operating in single pass through the vacuum system; and
2. Pulsed CRDS QCL spectrometer.

The data for the results presented here were obtained in real-time but post-processed using MATLAB®.

4.1. QCL pulsed laser spectrometer operating in single pass

Figure 6 shows results from the single pass measurements. The results were taken with either nitromethane, CH_3NO_2 or acetone, C_3H_6O in the vacuum system. The single pass measurements were performed by replacing one of the output couplers (the one closest to the MCT) with a calcium fluoride window. The QCL was operated at 100kHz repetition rate and 100ns pulse width. The results presented in Fig. 6 were recorded in real-time by multiplying the MCT signal with a 100kHz local oscillator using a Stanford Research Systems SR530 Analog lock-in amplifier.

#165708 - $15.00 USD Received 29 Mar 2012; revised 15 May 2012; accepted 12 Jun 2012; published 25 Jun 2012

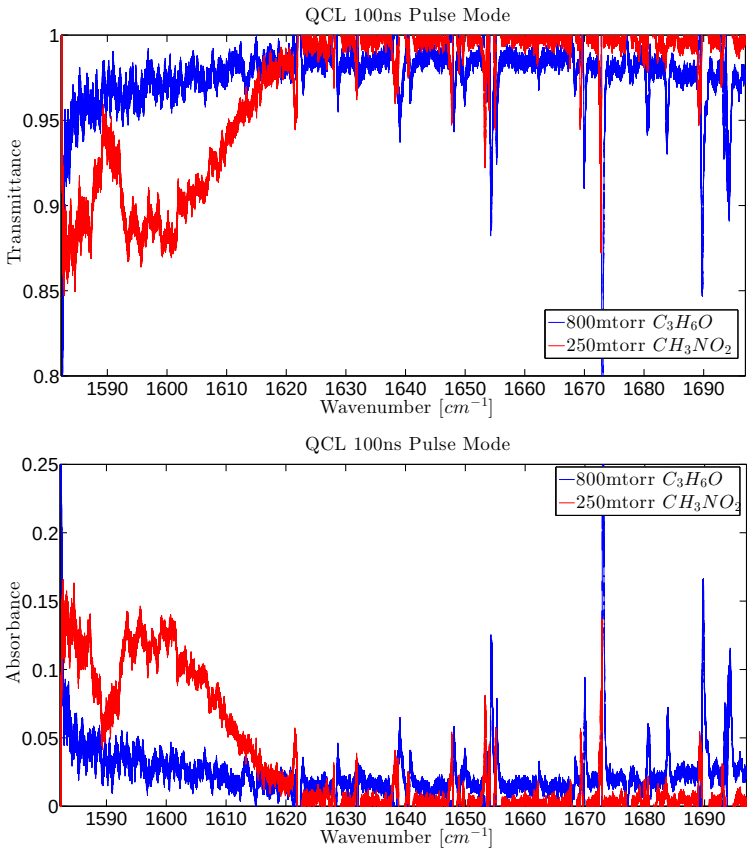

Fig. 6. Single pass measurements of nitromethane, CH_3NO_2 and acetone, C_3H_6O.

The single pass show both the transmittance and absorbance, see Eq. (3), of the chemicals for the nominal pressures of 800mTorr of C_3H_6O and 250mTorr CH_3NO_2. The results show that CH_3NO_2 predominantly absorbs in the 1582.25 cm^{-1} to 1620.00 cm^{-1} wavelength range, where as C_3H_6O absorbs in the 1582.25 cm^{-1} to 1620.00 cm^{-1} and 1660.00 cm^{-1} to 1697.00 cm^{-1} ranges. These measurements agree well with with data recorded on the National Institute of Advanced Industrial Science and Technology (AIST), Japan, database [27], and that reported by Beal *et. al.* [28]. Note that the wavelengths for the main absorption peaks for acetone, nitromethane and TNT are outside the wavelength range of this laser system. Also, the single pass spectrum of TNT was not measured because its absorbance was too small to be observed.

4.2. Pulsed CRDS QCL spectrometer

The QCL laser system was capable of rapidly scanning through its wavelength range, (0.2s to 7s sweep times) between 1582.25 cm^{-1} (6.3201μm) and 1697.00 cm^{-1} (5.8928μm), but for the results presented here we kept the scan rate constant at 7s.

Figure 7 shows CRDS signals with a 500ns pulse width and 100ns pulse width from the QCL, and a 100kHz repetition rate. The CRDS pulse train signals were measured on a Tektronix DPO4104 oscilloscope and analysed using MATLAB®. Note that the same frequency components can be observed compared to that of Fig. 4 but the magnitude of the harmonics differ. Furthermore, the CRDS signals measured are clearly noise limited from the time trace data, but the frequency harmonics are well above the noise floor, having an SNR $>$ 20 dB for

#165708 - $15.00 USD Received 29 Mar 2012; revised 15 May 2012; accepted 12 Jun 2012; published 25 Jun 2012

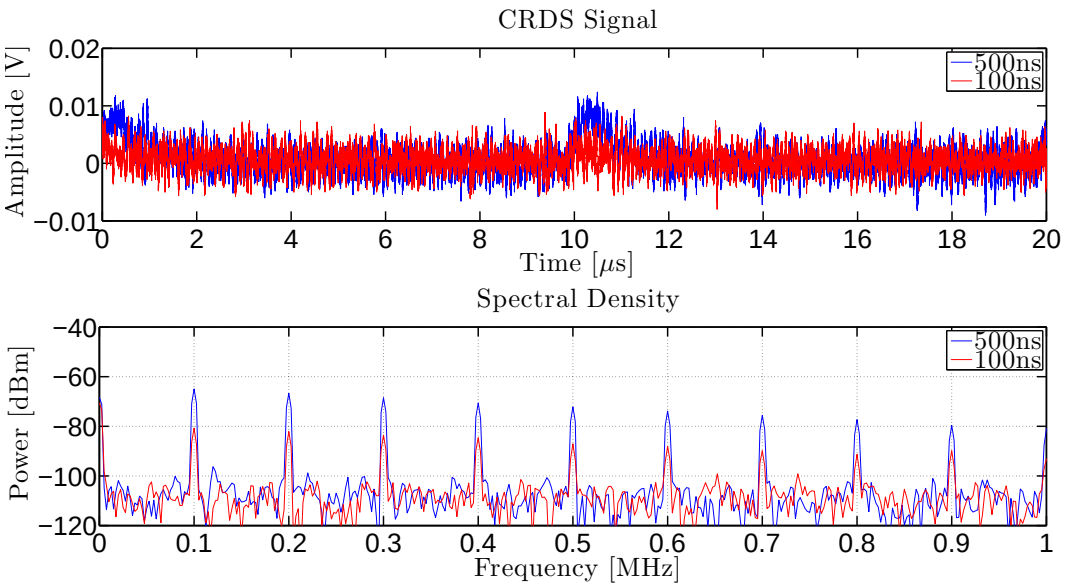

Fig. 7. CRDS signals as measured by the MCT on a Tektronix DPO4104 oscilloscope. The PSD was determined using the pwelch command in MATLAB®.

both pulse widths.

Although the data were recorded and analysed for both 500ns pulse width and 100ns pulse widths, the results presented here are from the 100ns data. The experimental differences with these data and those presented in Sec. 4.1 are the replacement of the 99.8 % output coupler, and the addition of a second Stanford Research Systems lock-in amplifier, SR844 DSP lock-in amplifier, to measure 200kHz component. The MCT signals were measured by both lock-in amps simultaneously, then the output was recorded by two channels from a National Instruments 100kHz DAQ. The data were then processed in real-time using LabVIEW, as well as recorded to disk to be later analysed using MATLAB®.

The important difference between this approach compared to others is that the data files recorded to disk for the 7s scans were $<$ 10MBits as opposed to the data files for a conventional CRDS system operating at 100MS/s and 10bit to gather $>$ 700MBits.

Figures 8, 9, 10, and 11 show results from real-time scans of nitromethane, acetone, nitromethane and acetone in room air, and trinitrotoluene, respectively.

Each figure contains three plots:

1. The raw data from the lock-in amplifier, as recorded by the DAQ operating at 100ks/s, of the power at the 100kHz fundamental. The data for the second harmonic is not displayed;
2. The power ratio of the second harmonic to fundamental, $\frac{f_2}{f_1}$; and
3. The absorbance determined from the data as outlined in Sec. 2.2.

Present in all plots are the absorbing features from the QCL passage through room air. The raw data plots have the same features as observed in Fig. 5. However, the presence of these external influences can clearly be distinguished from the species of interest as can be seen from the other two plots. The power ratio plots and absorbance plots both show that the room air features have a dispersion shape signature after processing, where as the features of interest have a monotonically increasing or decreasing signature.

#165708 - $15.00 USD Received 29 Mar 2012; revised 15 May 2012; accepted 12 Jun 2012; published 25 Jun 2012

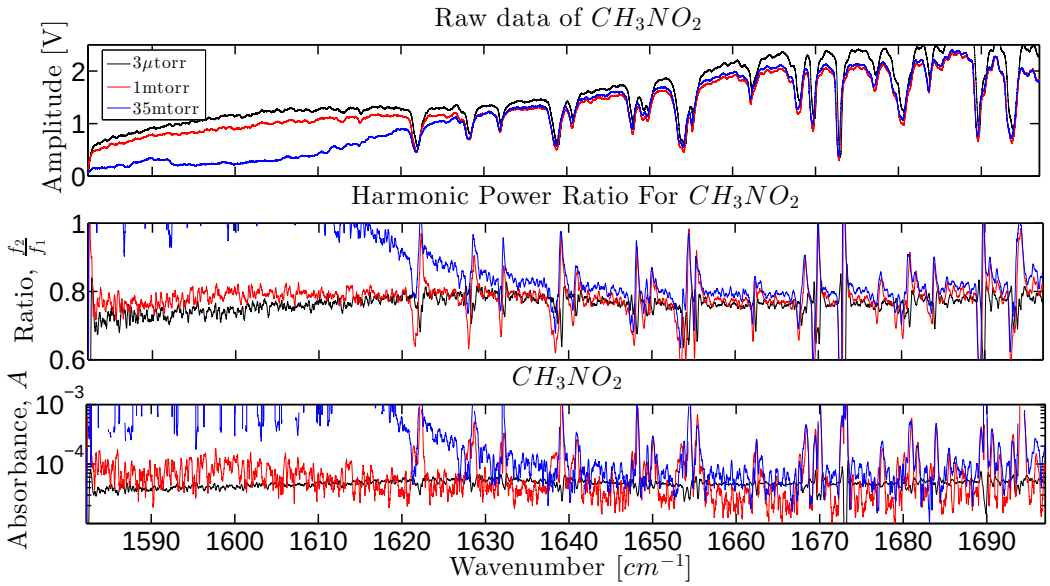

Fig. 8. Continuous wavelength spectrum measuring Nitromethane, CH_3NO_2, at various pressures.

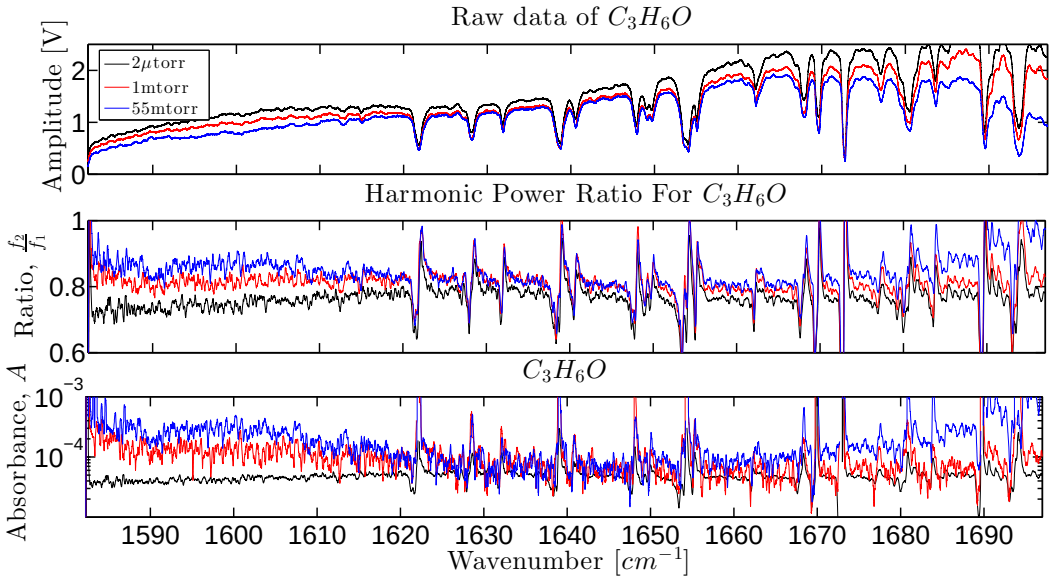

Fig. 9. Continuous wavelength spectrum measuring Acetone, C_3H_6O, at various pressures.

#165708 - $15.00 USD Received 29 Mar 2012; revised 15 May 2012; accepted 12 Jun 2012; published 25 Jun 2012

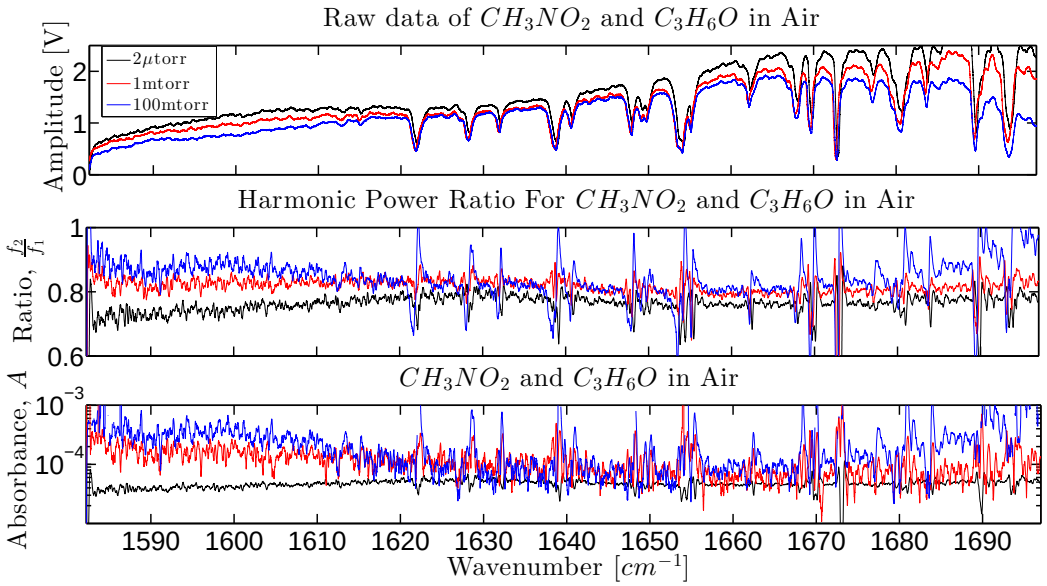

Fig. 10. Continuous wavelength spectrum measuring CH_3NO_2 and C_3H_6O combined with room air, at various pressures.

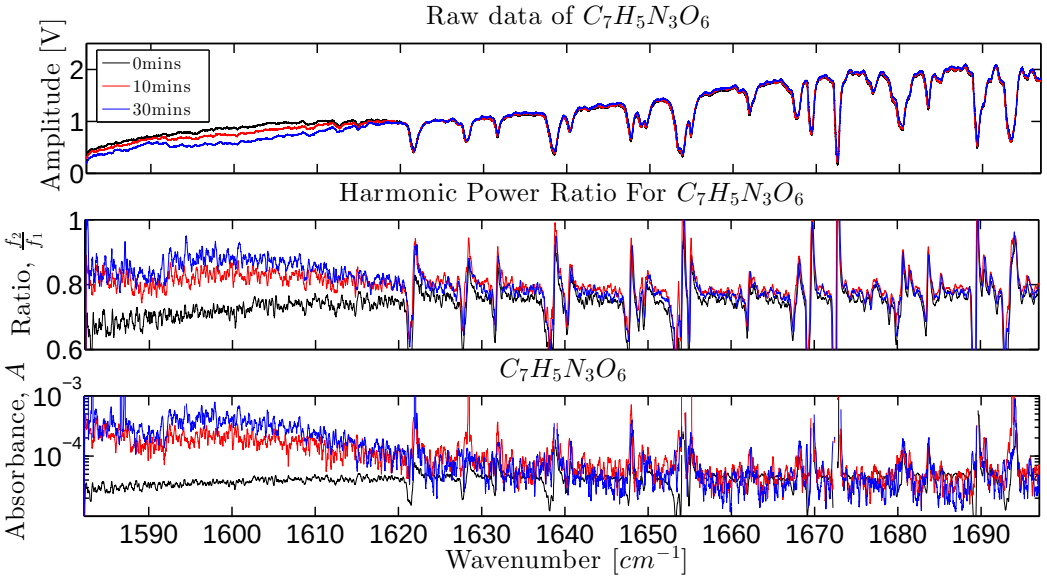

Fig. 11. Continuous wavelength spectrum measuring Trinitrotoluene, $C_7H_5N_3O_6$, at various equilibrium times.

#165708 - $15.00 USD Received 29 Mar 2012; revised 15 May 2012; accepted 12 Jun 2012; published 25 Jun 2012

Comparing the absorbance of CH_3NO_2 in the single pass measurements to that of the CRDS, at say 1600.00 cm^{-1}, we find that $A = 0.125$ for 250 mTorr and $A \approx 1 \times 10^{-4}$ for 1mTorr, where it should be ≈ 5 times larger than this value. Similarly for C_3H_6O, $A = 0.03$ at 800mTorr single pass and $A \approx 5 \times 10^{-4}$ for 1mTorr, where it should be ≈ 10 times smaller than this value. These discrepancies imply that the absolute calibration of the injected chemicals to the cell may have been faulty, and will be improved in future measurements.

Figure 11 shows the TNT data. In this case two 3mm$\times$1mm pieces of TNT were placed into the cell and allowed to come to an equilibrium pressure. The measurements were performed every 10 minutes for 90 minutes, and no change was noticed after 30 minutes. The TNT signal was clearly visible above the background and the results were reproducible. After 10 minutes the pressure in the cell was measure to be $\approx$ 1mTorr, and rose to $\approx$ 5 mTorr after 30 minutes.

5. Conclusion

The results presented in this paper, illustrate that real-time processing of CRDS signals is possible. They show that low finesse mirrors with 99.8% input/output coupling can be used with good sensitivity. Furthermore, the results show that medium to large molecules such as nitromethane, acetone, and TNT can be observed with good sensitivity using this wideband laser-based cavity ringdown spectrometer.

These results illustrate a methodology for the improved data processing capability needed to enable wideband laser-based cavity ringdown spectrometers, allowing them to compete strongly with standard FTIR instruments via their extreme cavity enhancement factors.

This paper presents preliminary results for the characteristics of a new QCL-based substance detection apparatus we have developed. We show that our new data processing technique allows gathering and analyzing CRDS data in real time, so that the full wavelength scanning capabilities of the new generation of QCL devices can be utilized to full advantage in cavity enhanced spectroscopic systems. We still face the challenge of current detector sensitivities and laser sources to reach the ultimate noise limits. Nevertheless, in future research we will develop the complete system to test modern estimation and control techniques in real time.

Acknowledgments

We would like to thank the Australian Federal Police, National Science Foundation (NSF Grant #: 0728285), The Louisiana Board of Regents and the Australian Research Council for their support of this research. We would also like to thank Prof. Chris Lennard, University of Canberra, Chris Armacost, Daylight Solutions and Peter Schulze, Los Alamos National Laboratory, for their help during this work.

#165708 - $15.00 USD Received 29 Mar 2012; revised 15 May 2012; accepted 12 Jun 2012; published 25 Jun 2012